Acoustoelectric Effect Study for SAW Sensors

D.C. Malocha and B. Fisher
School of Electrical Engineering & Computer Science
University of Central Florida, Orlando, Fl 32816
malocha@mail.ucf.edu

Abstract— **Research has recently begun on the use of ultra thin films and nanoclusters as mechanisms for sensing of gases, liquids, etc., since the basic material parameters may change due to film morphology. As films of various materials are applied to the surface of SAW devices for sensors, the conductivity of the films may have a strong acoustoelectric effect, whether desired or not. The purpose of this paper is to reexamine the theory and predictions of the acoustoelectric effect for SAW interactions with thin conducting or semi-conducting films. The paper will summarize the theory, and predict the effects of thin film conductivity on SAW velocity and propagation loss versus frequency and substrate material. The theory predicts regions of conductivity which result in extremely high propagation loss, which also correspond to the mid-point between the open and short circuit velocities.**

As an example of the verification and possible usefulness of the acoustoelectric effect, recent experimental results of palladium (Pd) thin films on an YZ $LiNbO_3$ SAW delay line have shown large changes in propagation loss, depending on the Pd film thickness, and/or exposure to hydrogen gas. By proper design, a sensitive hydrogen leak detector SAW sensor can be designed.

I. Introduction

In a piezoelectric semiconducting media, the piezoelectric effect will interact with the semiconducting media and affect acoustic wave propagation. This was first studied in the 1940's and began to be extensively studied in the 1960's. Most of the early studies were interested in elastic wave propagation interactions in semiconductor substrates and films. One of the earliest papers by Hutson and White in 1962 laid the mathematical foundation for the one dimensional propagating wave in a semiconducting solid [1]. In 1969, Ingebrigtsen considered attenuation of a SAW due to a semiconducting thin film [2]. The initial theoretical works with elastic wave and semiconductor interactions were motivated by the desire for providing useful amplification, but was abandoned since it was not practical. In 1972, Hemphill then assumed a similar set of equations could be applied to losses in thin metallic films [3]. In 1984, Hemphill reported further study of the effect of a SAW and thin film vanadium dioxide phase transition metal interaction for possible use in a programmable SAW delay line [4].

The purpose of this paper is to reexamine the theory and predictions of the acoustoelectric effect for SAW interactions with thin conducting or semi-conducting films. The motivation of the work was to investigate ultra-thin film interactions with gases and the environment. Film layers at the nano scale have differing properties than the conventional thin films, and their resistivity may be large and variable. The paper summarizes the theory, and predicts the effects of thin film conductivity on SAW velocity and propagation loss versus frequency and substrate material.

As an example of the usefulness of the acoustoelectric effect, recent experimental results of palladium (Pd) ultra-thin films on an YZ $LiNbO_3$ SAW delay line have shown large changes in propagation loss, depending on the Pd film thickness, and/or exposure to hydrogen gas. By proper design using ultra-thin Pd, the goal is to produce a passive, wireless, sensitive hydrogen leak detector SAW sensor.

II. Background Review of Acoustoelectric Effect

A. Theoretical Background

The following is a brief summary of the derivation of the acoustoelectric effect (AE). The initial approach presents a simple 1-D summary analysis of wave propagation which can be applied to SAW phenomenon, as derived in [1]. The approach assumes volume wave propagation in an isotropic media and allows the volume to be conductive and to interact with the wave. This substrate can have a resistivity between zero and infinity. The substrate material is also assumed piezoelectric which allows a travelling potential in synchronous with the wave.

Consider a wave propagating in the x direction. From classical physics, the force on a particle is the product of the mass times the acceleration. In the solid a similar relationship can be derived using the stress-strain relations and result in the following

$$\delta T/\delta x = \rho\, \delta^2 \mu/\delta t^2 \quad \text{and} \quad S = \delta\mu/\delta x \qquad (1)$$

where S is strain, T is stress, μ is displacement and ρ is the material mass density. Assume the substrate is characterized by a piezoelectric constant, e, and the strain, S, produces an electric field, $\mathcal{E}$, in x. For the one-dimensional problem, the constitutive relations are:

The authors acknowledge support through NASA-KSC STTR contract NNK07EA39C, Applied Sensor Research & Development Corp. (ASR&D), and the McKnight Doctoral Fellowship Program.

$$T = c^{\varepsilon} S - e\mathcal{E}$$
$$D = eS + \in \mathcal{E} \qquad (2)$$

where $\mathcal{E}$ is the electric field, c is the elastic constant at constant $\mathcal{E}$, and $\in$ is the dielectric permittivity at constant strain. From (2)

$$\frac{\delta T}{\delta x} = c\frac{\delta S}{\delta x} - e\frac{\delta \mathcal{E}}{\delta x}$$
$$\frac{\delta D}{\delta x} = e\frac{\delta S}{\delta x} + \in \frac{\delta \mathcal{E}}{\delta x} \qquad (3)$$

For a conductive volume, the current density yields

$$J = \frac{\delta D}{\delta t} = \sigma \cdot \mathcal{E} \qquad (4)$$

Assuming plane wave propagation, then $D = D_0 e^{j(kx-\omega t)}$ and $\mathcal{E} = \mathcal{E}_0 e^{j(kx-\omega t)}$, and equation (4) can be solved for D and $\mathcal{E}$ as

$$D = -j\frac{\sigma}{\omega} \cdot \mathcal{E} \qquad (5)$$

Substituting (5) into (2) and solving for $\mathcal{E}$ yields

$$\mathcal{E} = \frac{-\frac{e}{\in} \cdot S}{1 + j\frac{\sigma/\in}{\omega}} \qquad (6)$$

Define $f_r = \sigma/2\pi\in$ as the dielectric relaxation frequency, then substituting (6) into (2) and solving yields

$$T = c\left[1 + \frac{e^2}{c\in}\frac{\left(1 - j\,f_r/f\right)}{1 + \left(f_r/f\right)^2}\right] \cdot S \qquad (7)$$

or

$$T = c_{eff} \cdot S$$

Assuming plane wave propagation as before, then $\mu = \mu_0 e^{j(kx-\omega t)}$ and

$$-\rho\omega^2\mu = -c_{eff} \cdot k^2 \cdot \mu \qquad (8)$$

Since the effective stiffness constant is complex, and frequency is real, then the wave number, k, is complex. This implies a decaying propagating wave in the x-direction. The velocity must be real and is given as

$$v = \mathrm{Re}\left(\omega/k\right) = \sqrt{\frac{c}{\rho}\left[1 + \left(\frac{e^2}{c\cdot\in}\right)\left(\frac{1}{1 + \left(f_r/f\right)^2}\right)\right]} \qquad (9)$$

The propagation loss coefficient, α, is given by

$$\alpha = \mathrm{Im}(\omega/k) = \omega \cdot IM\left(\sqrt{\rho/c_{eff}}\right)$$

$$\alpha \approx \frac{\omega}{v_0}\frac{e^2}{2c\in}\left(\frac{\left(f_r/f\right)}{1 + \left(f_r/f\right)^2}\right) \qquad (10)$$

Next, Ingebrigtsen similarly solved the 2-D equations for a SAW propagating in the x-direction, depicted in Fig. 1, interacting with a thin resistive film on the surface of a piezoelectric material [2]. The half-space below the piezoelectric substrate is assumed as free space, but could be another dielectric. The resulting equations are the same with substitution of the following:

$$\in = \in_0 + \in_p \quad \text{and} \quad \in_p = \left(\in_{11}\in_{22} - \in_{12}^2\right)^{1/2} \qquad (11)$$

Figure 1 SAW propagation schematic for analysis.

B. AE Discussion and Results

The AE theory predicts a relaxation frequency which is the frequency where maximum SAW attenuation will occur. The relaxation frequency is inversely proportional to the material's dielectric constant and thin film resistivity, but independent of material coupling coefficient. Changing the substrate or free space dielectric constant, or the film resistivity will change the relaxation frequency. A plot is shown in Fig. 2 of the relaxation frequency for three relative dielectric constants as a function of thin film resistivity.

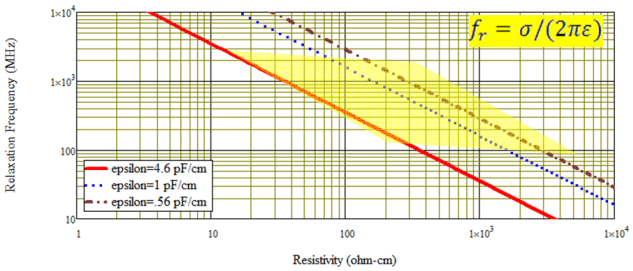

Figure 2 Relaxation frequency versus thin film resistivity for three dielectric constants, typical of common SAW substrates. The shaded area is typical range of SAW device operation.

Fig. 3 shows the effect of film resistivity on propagation loss and velocity for a SAW on YZ $LiNbO_3$. The propagation loss peak occurs at a specific resistivity value where the SAW operational frequency equals the relaxation frequency; at maximum attenuation the propagation velocity is also midway between the open and short circuit velocity. The AE velocity shift is greatest on high coupling materials; at 500 MHz being less than 0.1 ppm on quartz but greater than 200 ppm on YZ $LiNbO_3$. The fractional velocity change being greatest at the peak attenuation is unfortunate for many applications.

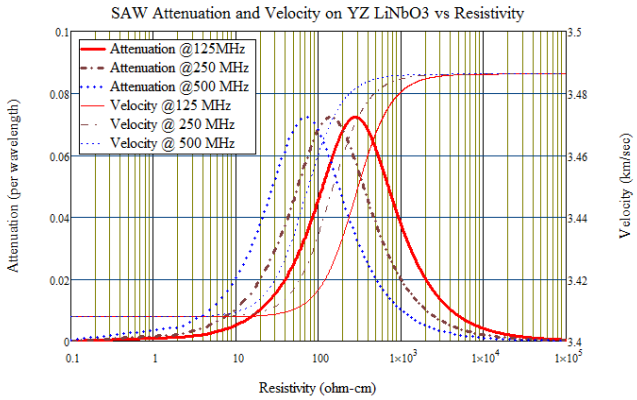

Figure 3 Predicted SAW attenuation per wavelength and velocity versus resistivity for YZ LiNbO3. Three SAW center frequencies, 125, 250 and 500 MHz are shown.

Figure 4 shows the YZ $LiNbO_3$ propagation loss in dB/cm for 125, 250, and 500 MHz operation; providing a more physical interpretation. The peak attenuation rises rapidly with frequency and is strongly thin film resistivity dependent. To traverse the high loss region, from the open to short circuit velocity, a film resistivity will need to change over several orders of magnitude with a change in the desired sensor measurand.

The SAW propagation losses are so high, that it is useful to expand Fig. 4 into the low resistivity region, as shown in Fig. 5. At low frequencies, thin film losses are negligible, but as frequency increases the loss can be appreciable, depending on device length and thin film thickness.

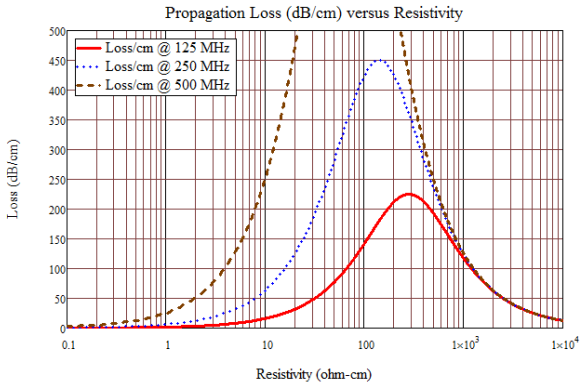

Figure 4 Propagation loss (dB/cm) versus resistivity (ohm-cm) for YZ LiNbO3 at 125, 250, and 500 MHz.

C. Early Experimental Work

Given the theoretical background, early investigations were conducted by many researchers on many different waves, materials and embodiments. R. B. Hemphill, first in 1972 and then in 1984 [3,4], studied the SAW AE effect on SAW materials still used today, quartz and lithium niobate substrates. His earliest work investigated thin metal film and SAW interactions and showed good correlation between his theory and experiments. An example figure from his work is shown in Fig. 6; a plot of attenuation versus sheet resistivity for a gold film on YZ $LiNbO_3$.

In 1984, Hemphill investigated thin film transition metals effects on SAW propagation for the possible use in programmable devices. He recognized that some transition metals can have large changes in resistivity versus the external environment and this could be used as an environmentally programmable element by noting the change in the SAW velocity or delay. He showed experimental results for vanadium dioxide films, and found good correlation to his predictions.

Since the early investigations, there has been a wealth of research on the SAW AE effect on metals, oxides and overlay layers. The previous discussion and presentation provides a foundation for the current efforts.

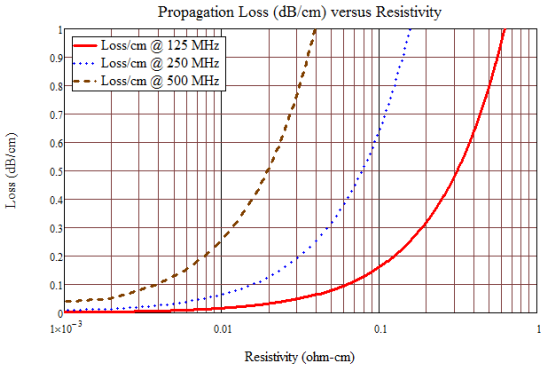

Figure 5 Propagation loss (dB/cm) versus resistivity (ohm-cm) for YZ LiNbO3 at 125, 250, and 500 MHz.

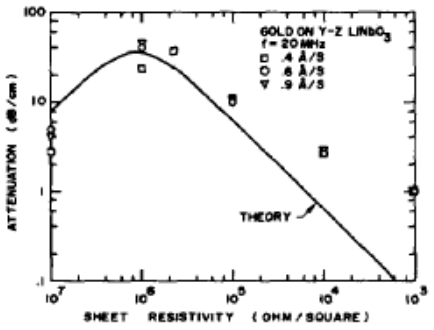

Fig. 5. Attenuation at 20 MHz as a function of sheet resistance for gold deposited at 0.4, 0.6, and 0.9 Å/sec.

Figure 6 An example (Fig. 5) from R.B. Hemphill [3]; a plot of attenuation (dB/cm) versus sheet resistivity (ohm/square) for a gold film on YZ $LiNbO_3$ at 20 MHz.

III. Palladium Ultra-Thin Film Effects

A. Sensor Application

The ultimate goal of the research is to produce a wireless, passive gas hydrogen sensor. One basic embodiment is shown in Fig. 7, where a Pd thin film is placed in the propagation path between a transducer and an orthogonal frequency coded (OFC) reflector that can affect the amplitude or delay of the reflected signal. A second OFC reflector has no Pd film in the path and acts as a reference. In order to build an operational device, first the Pd film needs investigation and then the SAW Pd-film interaction needs to be characterized.

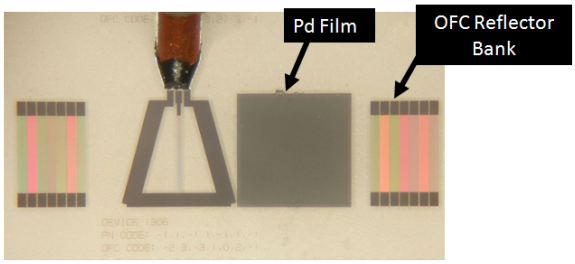

Figure 7 Example SAW OFC RFID hydrogen sensor embodiment. The device is being tested on an RF probe station and the reflector diffraction pattern is apparent from the OFC reflectors at differing frequencies.

B. Pd Ultra-Thin Film Background Discussion

The use of SAW devices as sensors was introduced in the 1970's and continues to be explored to date. The use of SAW and Pd thin films for use as sensors has also had a wealth of publications to date and only a few examples are referenced here. It has been recognized that Pd absorbs hydrogen and that this absorption may change the mechanical or AE parameters of the SAW-film interaction.

The focus of this Pd thin film research was to characterize films in the ultra-thin film range, from approximately 1-10 nm in thickness. Almost all previous publications on SAW Pd hydrogen sensors have had films in the 10-1000 nm thickness range [5,6,7]. Thin films in the nano-meter thickness range can behave much differently than thicker films due to film morphology, different physical conduction mechanisms, and different gas interactions. The films have very small volume, which allows hydrogen gas to diffuse in and out very rapidly. If there is a binding to form Pd hydride, then the reaction rate should also be very rapid. Depending on the Pd-gas interaction, the resistivity will change rapidly and may be reversible [8], 9]. If the film is operating in the high resistivity range, it may be possible for a large resistivity change due to the "swelling" of Pd nano-clusters. The purpose of this work is to study the ultra-thin film Pd films, using the AE effect to increase the sensitivity of the gas, film and SAW interaction.

C. Pd Thin Film Experimental Study

Pd thin films were deposited using an electron beam evaporation system. A base pressure of approximately 10^{-6} Torr was achieved before evaporation. A quartz crystal thickness monitor is used to record the inferred metal thickness and is located in close proximity to the samples. The thickness is inferred by the mass change on the quartz crystal microbalance of the deposited Pd film. Since the films are ultra-thin, it is expected that the film morphology will not necessarily be uniformly amorphous. Rather it is expected that the film may form cluster sites of varying sizes dependent on the substrate, substrate pre-deposition process, and Pd deposition conditions. The thickness monitor was calibrated as carefully as possible to attempt reproducibility and accuracy. Many deposition runs were used to remove sources of error, and many more deposition runs were made to verify reproducibility. Fig. 8 shows a typical data run of the measurement of Pd film resistivity versus thickness. The curve is obtained under vacuum by measuring the resistivity between two thin film metal plates of gold. The in-situ measurement is recorded using a programmable multimeter and deposition monitor. The deposition rate is maintained at approximately 0.1 A°/sec. The plot shows an exponential change in resistivity versus film thickness when films are less than approximately 50 A° and the thin film resistivity is within the range of interest, as shown in Fig. 3. This is fortuitous for possible use as sensors if the hydrogen gas can affect the films properties.

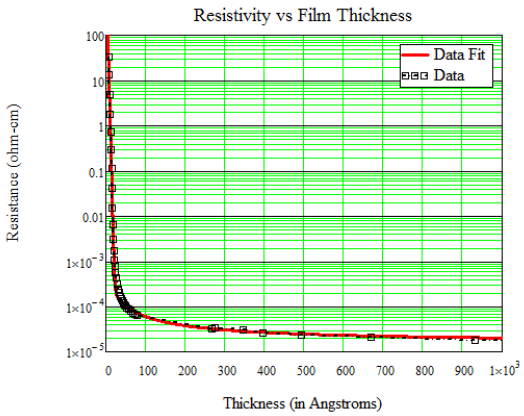

Figure 8 In-situ vacuum, measured Pd film resistivity versus thickness, as inferred from mass loading on quartz resonator of crystal monitor.

D. SAW Pd Thin Film Experimental Results

In order to examine the affects of the SAW-Pd thin film interaction, with and without hydrogen exposure, a series of test devices were designed and fabricated. The devices presented were fabricated on YZ $LiNbO_3$ substrates at approximately 123 MHz. The structures were made of aluminum films with the transducer sampled at $4*f_0$ and the reflector was composed of 25, ¼ wavelength shorted electrodes. Three devices were tested, a control wafer without a Pd film, and two designs having Pd either in the propagation path or atop of the reflector. The Pd-path device provides propagation loss data while the Pd-reflector response would yield a change in the shorting of the Al structure. The devices S_{21} frequency responses were obtained via an RF probe station and network analyzer and then transformed into the time domain; the reflector time response is shown in Fig. 9. The control device without Pd showed the lowest loss of approximately 23 dB, the device with Pd in the propagation path had approximately 45 dB loss, and the device with Pd on the reflector had approximately 31 dB loss. The Pd film length was 1.27 mm in the propagation direction, yielding a loss of approximately 86 dB/cm. The Pd thin film thickness is estimated at approximately 15 A^o, based on the in-situ thin film resistivity measurements.

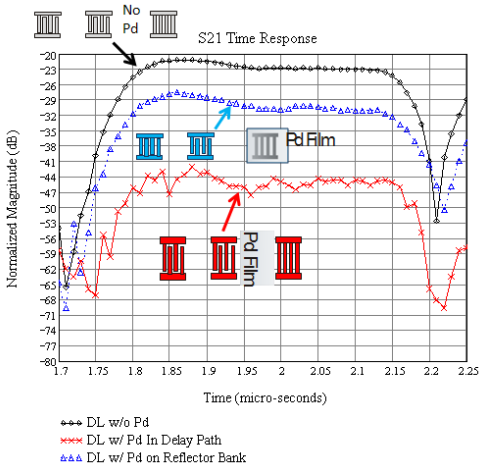

Figure 9. Plots of the S_{21} time domain reflector response of a simple delay line on YZ $LiNbO_3$ for three cases: 1) control device without Pd film, 2) device with Pd film on the Al reflector grating and 3) device with Pd film in the propagation path.

Next, the devices with the Pd films were exposed multiple times to a 2% hydrogen and 98% nitrogen gas mixture. The gas exposure was accomplished on the RF probe station via a small poly tube to deliver the gas to the substrate area. The films reacted immediately to gas exposure, as recorded by sight. As seen, multiple gas exposures resulted in decreasing measured loss; approaching that of the control device. The change in insertion loss for the Pd-delay path device is approximately 20 dB and the propagation loss is now only 7.8 dB/cm; seen in Fig. 10. The change in insertion loss for the Pd-reflector device is approximately 7 dB, seen in Fig. 11. At room temperature, the devices showed no reversibility

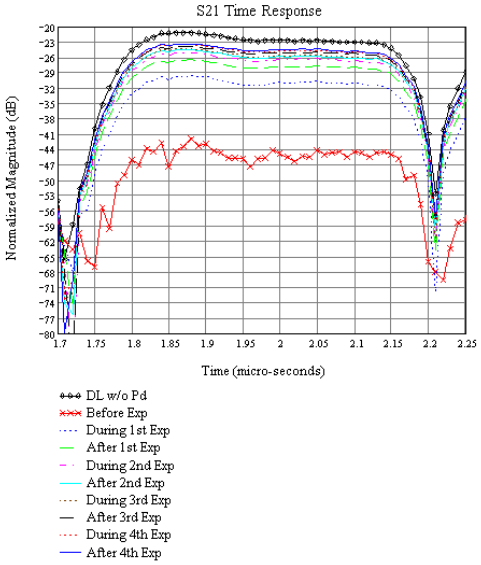

Figure 10. Plots of the S_{21} time domain reflector response of a simple delay line on YZ $LiNbO_3$. Control device has lowest loss as reference. Curves show effect of multiple 2% hydrogen exposures.

back to their pre-hydrogen exposure operational levels. However, both device structures show strong sensitivity to hydrogen gas exposure and could be used as an on-off gas sensor when integrated into a wireless SAW sensor embodiment.

IV. Discussion and Conclusions

This paper presented background on the pioneering work on the acoustoelectric effect for SAW devices. They provided the theoretical basis and the earliest experimental

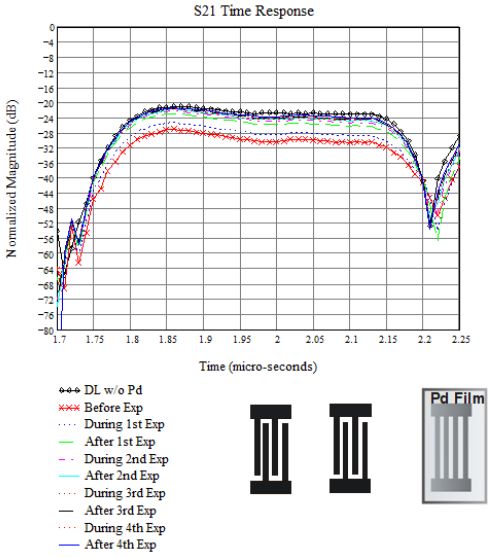

Figure 11. Plots of the S_{21} time domain reflector response of a simple delay line on YZ $LiNbO_3$. Control device has lowest loss as reference. Curves show effect of multiple 2% hydrogen exposures.

verification, as well as some of the first sensors. Experimental measurements of Pd thin film resistivity have been shown and initial experimental results on SAW-Pd propagation loss are presented. The measurements of propagation loss verified a large propagation loss effect, as predicted by the AE theory.

The initial results of the SAW device exposure to hydrogen gas imply an approximately equivalent 10x change in the Pd thin film resistivity. This is an unexpectedly large change in resistivity, which could suggest a significant change in film morphology. One explanation could be an expansion of the Pd film parallel to the surface which would enhance the thin film percolation effect and reduce the film resistivity. The increase in conductivity may also be due to quantum mechanical enhanced electron tunneling, or by physical connectivity increases due to film displacement upon exposure. The films have not yet been inspected or characterized for initial morphology or for post gas exposure morphology.

The large change in SAW propagation loss with only 2% hydrogen gas exposure demonstrates a very large sensitivity, ideal as a sensor. A SAW device embodiment operating in a differential mode with Pd in one path could operate as a warning "switch" sensor. The 2% hydrogen gas concentration is below the ignition threshold, which is often important for such a sensor. The ultimate sensitivity to both low and high hydrogen gas concentrations needs further investigation.

These are initial device results and are extremely encouraging, but leave many questions unanswered. Device fabrication processes are critical for Pd hydrogen sensitivity due to thin film changes at growth. The devices currently operate irreversibly at room temperature, but perhaps reversibility is achievable with different film morphology. The film and device physics needs further work to understand all the mechanisms causing the SAW film interactions. It is noteworthy to realize that the SAW device is a contactless method to evaluate thin film properties and itself, is a sensor that may be very useful. Both the Pd film conductivity and dielectric properties require further study. The SAW/Pd interaction occurs at the micron and sub-micron level due to the SAW wavelength and the film morphology. The frequency dependent effects need further study with the goal of a sensitive, reversible room temperature SAW wireless, passive hydrogen gas sensor.

ACKNOWLEDGMENT

The authors are most grateful to Dr. Robert Youngquist, NASA-KSC for his continuing support discussions and suggestions. The authors acknowledge support through NASA KSC STTR contract NNK07EA39C, Applied Sensor Research & Development Corp. (ASR&D), and the McKnight Doctoral Fellowship.

REFERENCES

[1] A.R. Hutson and D.L. White, "Elastic Wave Propagation in Piezoelectric Semiconductors", J. of Applied Physics, Vol. 33, no. 1, Jan. 1962, pp. 40-47.

[2] K.A. Ingebrigtsen, "Linear and Nonlinear Attenuation of Acoustic Surface Waves in a Piezoelectric Coated with a Semiconducting Film", J. of Applied Physics, Vol. 41, n0. 2, Feb. 1970, pp. 454-459.

[3] R.B. Hemphill, "Attenuation of Surface Waves on a Piezoelectric Coated with Thin Metal Films", 1972 IEEE Ultrasonics Symposium Proceedings, pp. 340-342.

[4] R.B. Hemphill, "Effect of a Thin-Film Phase-Transition Metal on Surface Acoustic Wave Propagation", 1984 IEEE Ultrasonics Symposium Proceedings, pp. 1006-1010.

[5] A. D'Amico, A. Palma, and E. Verona, "Hydrogen Sensor Using a Palladium Coated Surface Acoustic Wave Delay-Line," IEEE Ultrasonics Symposium, pp. 308-311, 1982.

[6] A. D'Amico, A. Palma, and E. Verona, "Palladium-surface acoustic wave interaction for hydrogen detection," Applied Physics Letters, vol. 41, pp. 300-301, 1982.

[7] Jakubik, W.P. , Urbanczyk, M.W. , Kochowski, S., Bodzenta, J., "Palladium and phthalocyanine bilayer films for hydrogen detection in a surface acoustic wave sensor system", Sensors and Actuators B: Chemical. Vol. B96, no. 1-2, pp. 321-328. 15 Nov. 2003.

[8] O. Dankert and A. Pundt, "Hydrogen-induced percolation in discontinuous films", Appl. Phys. Lett. 81, 1618 (2002).

[9] T. Xu, M. P. Zach, Z. L. Xiao, D. Rosenmann, U. Welp, W. K. Kwok, and G. W. Crabtree, "Self-assembled monolayer-enhanced hydrogen sensing with ultrathin palladium films," Applied Physics Letters, vol. 86, pp. 203-204, 2005.